

Correlation between the quenching of total GT_+ strength and the increase of E2 strength

N. Auerbach^a, D.C. Zheng^b, L. Zamick^c and B.A. Brown^d

^a School of Physics and Astronomy, Tel-Aviv University, Tel Aviv 69978, Israel

^b Department of Physics, University of Arizona, Tucson, AZ 85721, USA

^c Department of Physics and Astronomy, Rutgers University, Piscataway, NJ 08855, USA

^d Department of Physics and Astronomy, Michigan State University, East Lansing, MI 48824, USA

Received 27 January 1993

Relations between the total β_+ Gamow–Teller (GT_+) strength and the E2 strength are further examined. It is found that in shell-model calculations for $N = Z$ nuclei, in which changes in deformation are induced by varying the single-particle energies, the total GT_+ or GT_- strength decreases monotonically with increasing values of the $B(E2)$ from the ground state to the first excited $J^\pi = 2^+$ state. Similar trends are also seen for the double GT transition amplitude (with some exceptions) and for the spin part of the total M1 strength as a function of $B(E2)$.

1. Introduction

In ref. [1] a relation between the $B(E2)$ value from the ground state to the first excited $J^\pi = 2^+$ state and the quenching of Gamow–Teller (GT) strength has been pointed out. The quenching we will discuss here is caused by those nuclear structure effects that do *not* affect the sum rule:

$$B_t(GT_-) - B_t(GT_+) = 3(N - Z), \quad (1)$$

where $B_t(GT_-)$ and $B_t(GT_+)$ are the (p, n) β_- and (n, p) β_+ GT transition strengths. (We will refer to the quenching of the sum rule value as the quenching due to the renormalization of the GT operator.)

The reduction of the total GT strength, discussed here, is such that it affects the total GT_+ and GT_- strengths in the *same additive* way and, therefore, cancels out when the difference $B_t(GT_-) - B_t(GT_+)$ is taken. Because of the Pauli blocking, in nuclei with a neutron excess, the β_+ branch (σt_+) of a GT transition is usually much weaker than the β_- branch. Hence, when the above mentioned quenching occurs, it is more pronounced in the β_+ transition.

The quenching of the total GT_+ strength, which concerns us, is due to the presence of multi-particle, multi-hole components in the wave function of the

initial and final states, i.e. $np-nh$ with $n > 2$. In a deformed nucleus, the amount of $np-nh$ admixture is large, so that the $2p-2h$ space is not sufficient to describe the ground state or transitions from the ground state to the GT states. A full shell-model calculation in an extended space is expected to predict the amount of quenching of the GT strength [2]. However, the possibility of performing such extended shell-model calculations is limited to very few cases. Various approximation schemes, such as the RPA and, more widely used in this context, the QRPA, describe well only the $2p-2h$ part of the $np-nh$ space. Consequently, it is important to try and develop a procedure that would enable us to predict the quenching of the GT strength, by finding a relationship of the GT strength to some other observable that is more easily accessible experimentally or theoretically.

Deformed nuclei have large $B(E2)$ values. This consideration should provide a simple indication of possible correlations between the quenching of the GT strength and the $B(E2)$ values. In ref. [1], such a relationship was suggested and tested for the case of ^{26}Mg , for which a full sd -space shell-model calculation is still possible. It was found that the total GT_+ strength is a monotonically descending function of the $B(E2)$ value for the transition from the ground state

to the first excited $J^\pi = 2^+$ state of the parent nucleus. This relation was then used in ref. [1] to estimate the total GT strength in the ^{54}Fe region.

In the present paper, we extend these calculations to more cases where one is able to perform large-space shell-model calculations of the total GT strength. The purpose is to confirm the previous conjecture about the above relationship between the total GT_+ or GT_- strength and the $B(E2)$ value, to provide more insight into the origin and to set some limits on the application of this relationship.

2. The calculation

Two of the few nuclei that are available for a complete space calculation are ^{20}Ne and ^{44}Ti . For these two nuclei, the GT_- and GT_+ strengths are equal and, therefore, the quenching will affect the two branches to the same degree. In ^{20}Ne , we allow the two valence protons and two valence neutrons to occupy the complete sd shell ($d_{5/2}$, $s_{1/2}$ and $d_{3/2}$), while in ^{44}Ti the two valence protons and two valence neutrons are allowed to occupy the complete fp shell ($f_{7/2}$, $p_{3/2}$, $f_{5/2}$ and $p_{1/2}$). The calculations are performed with two-body interactions used in previous calculations to describe the structure of these nuclei. In ^{20}Ne we use the Wildenthal interaction [3], while in ^{44}Ti two sets of matrix elements are used, the modified renormalized Kuo–Brown (MKB) interaction [4] and the FPD6 interaction [5]. As for single-particle energies, we use, in ^{20}Ne , the set (given in MeV)

$$\begin{aligned}\epsilon_{d_{5/2}} &= 0.0, \\ \epsilon_{s_{1/2}} &= 0.78(1+x), \\ \epsilon_{d_{3/2}} &= 5.59(1+x); \end{aligned} \quad (2)$$

and in ^{44}Ti we use, with the MKB,

$$\begin{aligned}\epsilon_{f_{5/2}} &= 0.0, \\ \epsilon_{p_{3/2}} &= 2.1(1+x), \\ \epsilon_{f_{7/2}} &= 4.4(1+x), \\ \epsilon_{p_{1/2}} &= 8.2(1+x), \end{aligned} \quad (3)$$

and, with the FPD6,

$$\begin{aligned}\epsilon_{f_{5/2}} &= 0.0, \\ \epsilon_{p_{3/2}} &= 1.89(1+x), \\ \epsilon_{f_{7/2}} &= 3.91(1+x), \\ \epsilon_{p_{1/2}} &= 6.49(1+x). \end{aligned} \quad (4)$$

The variable x is a parameter that will enable us to vary the single-particle spacing and, in particular, the spin–orbit splitting. In this manner we are also able to change the nuclear deformation. The value $x = 0$ corresponds to the realistic case used with the above two-body interactions to reproduce the empirical properties of the nuclei under discussion.

It is also instructive to look at the $\text{SU}(3)$ limit [6] for these nuclei, by constructing, in this limit, their wave functions and computing their $B(E2)$ values. In the $\text{SU}(3)$ limit, the total GT_+ and GT_- strengths from the ground state of an $N = Z$ nucleus vanish.

In the $\text{SU}(3)$ model, the spin–orbit splitting is put to zero, so that the spin–orbit partners are degenerate. The spacing between the single-particle states that are not spin–orbit partners are non-zero but have definite values, as given by the diagonal matrix elements of the Elliott, say, quadrupole–quadrupole ($Q \cdot Q$) interaction.

3. Results

Our calculated results are given in table 1 for ^{20}Ne and in table 2 for ^{44}Ti . In addition to the total GT_+ strength $B_t(\text{GT}_+)$, which we will discuss first, the results for many other quantities for different values of the spin–orbit splitting parameter x are also given in the tables.

In the pure configuration limit ($x \rightarrow \infty$), in both ^{20}Ne and ^{44}Ti , the total GT_+ strength $B_t(\text{GT}_+)$ is equal to 6.0. As configuration mixing is introduced, $B_t(\text{GT}_+)$ is reduced. In the realistic case (i.e. $x = 0$), it is reduced to about 0.55 in ^{20}Ne and to 1.88 with the MKB (1.27 with the FPD6) in ^{44}Ti .

As the parameter x is increased, the spacing between the lowest single-particle state ($d_{5/2}$ in ^{20}Ne and $f_{7/2}$ in ^{44}Ti) and other single-particle states is increased and the states approach the limit of the pure configurations. The $B(E2)$ values to the first excited $J^\pi = 2^+$ state $B_1(E2)$ decrease, and, at the same time,

Table 1

The GT_+ , M1 and E2 transition strengths from the ground state in ^{20}Ne as a function of x , a parameter signifying the splitting between the single-particle energy of the $d_{5/2}$ orbit and those of the $s_{1/2}$ and $d_{3/2}$ orbits (see text for more details). The calculations were performed in the full sd space, using the two-body matrix elements of the Wildenthal interaction [3]. In the table, Q is the quadrupole moment of the $J^\pi = 2^+, T = 0$ state and A_1 (DGT) is the ground state to ground state DGT amplitude. M1 strengths are in units of μ_N^2 and E2 strengths are in units of $e^2 \text{fm}^4$.

x	$B_t(GT_+)$ ^{a)}	$B_s(M1)$ ^{b)}	$B_o(M1)$ ^{c)}	$B_t(M1)$ ^{d)}	$B_1(GT_+)$ ^{e)}	$B_1(M1)$ ^{f)}	$B_1(E2)$ ^{g)}	Q ^{h)}	A_1 (DGT) ⁱ⁾
-1.0	0.116	0.305	1.487	1.781	0.000	0.566	298.4	-15.78	-0.051
-0.5	0.235	0.620	1.356	1.942	0.050	1.363	307.2	-16.07	-0.025
0.0	0.548	1.449	1.203	2.566	0.143	1.962	303.0	-15.81	0.246
0.5	0.949	2.508	1.075	3.439	0.241	2.412	291.2	-15.21	0.486
1.0	1.360	3.595	0.973	4.375	0.332	2.755	276.2	-14.36	0.702
1.5	1.739	4.596	0.889	5.255	0.409	3.007	260.7	-13.27	0.883
2.0	2.065	5.460	0.819	6.025	0.471	3.182	245.6	-11.97	1.028
4.0	2.880	7.612	0.643	7.967	0.589	3.427	197.7	-5.920	1.350
8.0	3.423	9.050	0.520	9.290	0.631	3.450	153.1	1.108	1.525
SU(3)	0.000	0.000	1.091	1.091	0.000	1.091	346.3	-17.07	0.000

^{a)} $B_t(GT_+)$: Total GT_+ strength to $J^\pi = 1^+, T = 1$ states.

^{b)} $B_s(M1)$: Total spin M1 strength to $J^\pi = 1^+, T = 1$ states.

^{c)} $B_o(M1)$: Total orbital M1 strength to $J^\pi = 1^+, T = 1$ states.

^{d)} $B_t(M1)$: Total M1 strength to $J^\pi = 1^+, T = 1$ states.

^{e)} $B_1(GT_+)$: GT_+ strength to the lowest $J^\pi = 1^+, T = 1$ state.

^{f)} $B_1(M1)$: M1 strength to the lowest $J^\pi = 1^+, T = 1$ state.

^{g)} $B_1(E2)$: E2 strength to the lowest $J^\pi = 2^+, T = 0$ state.

^{h)} Q : Quadrupole moment of the lowest $J^\pi = 2^+, T = 0$ state.

ⁱ⁾ A_1 (DGT): DGT amplitude for the transition $^{20}\text{O}(J^\pi = 0^+, T = 2) \rightarrow ^{20}\text{Ne}(J^\pi = 0^+, T = 0)$.

Table 2

Same as table 1 but for the transitions from the ground state in ^{44}Ti . The calculations were performed in the full fp space using the two-body matrix elements of the MKB [4] and of the FPD6 [5] interactions.

Interaction	x	$B_t(GT_+)$	$B_s(M1)$	$B_o(M1)$	$B_t(M1)$	$B_1(GT_+)$	$B_1(M1)$	$B_1(E2)$	Q	A_1 (DGT)
MKB	-1.0	0.095	0.252	2.713	2.985	0.006	0.551	829.3	-25.99	0.220
	-0.5	0.723	1.911	2.266	4.134	0.289	3.097	782.7	-24.61	0.679
	0.0	1.884	4.981	1.661	6.487	0.509	3.902	624.8	-14.97	1.103
	0.5	2.667	7.051	1.240	8.087	0.529	3.706	484.4	-0.923	1.257
	1.0	3.068	8.111	1.030	8.928	0.521	3.583	414.2	6.043	1.287
	1.5	3.289	8.696	0.921	9.409	0.514	3.522	382.4	9.038	1.282
	2.0	3.416	9.058	0.859	9.717	0.509	3.488	365.9	10.56	1.269
	4.0	3.672	9.706	0.762	10.30	0.496	3.437	341.9	12.71	1.222
FPD6	-1.0	0.040	0.107	2.881	2.988	0.000	0.401	835.6	-26.40	0.058
	-0.5	0.376	0.995	2.631	3.596	0.154	2.603	804.4	-25.64	0.283
	0.0	1.269	3.354	2.126	5.416	0.403	3.841	697.8	-21.61	0.809
	0.5	2.125	5.617	1.657	7.219	0.495	3.816	580.5	-13.12	1.176
	1.0	2.677	7.076	1.359	8.407	0.484	3.462	490.6	-4.184	1.367
	1.5	3.010	7.957	1.185	9.143	0.461	3.204	434.3	1.629	1.462
	2.0	3.222	8.516	1.081	9.621	0.442	3.039	401.1	4.984	1.512
	4.0	3.603	9.523	0.911	10.52	0.402	2.758	351.1	9.846	1.571
SU(3)		0.000	0.000	1.563	1.563	0.000	1.563	1067	-29.78	0.000

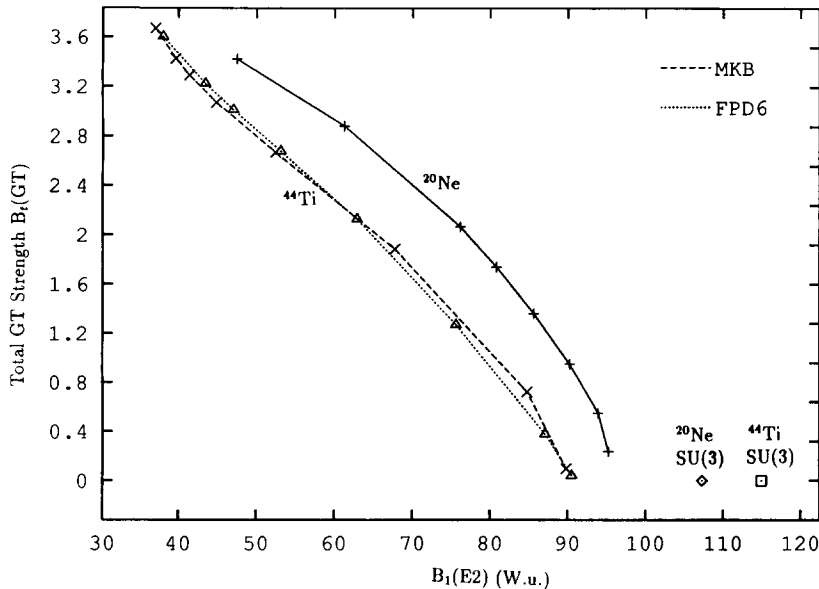


Fig. 1. The total GT_+ or GT_- strength from the ground states in ^{20}Ne (using the Wildenthal interaction) and in ^{44}Ti (using the MKB and the FPD6 interactions) as a function of the $B(E2)$ values from the ground state to the first excited $J^\pi = 2^+$ state in the Weisskopf units. The symbols “+”, “x”, “ Δ ”, etc. signify the points for which actual calculations were performed. The results in the SU(3) limit are also marked.

the total GT_+ strength $B_i(GT_+)$ increases monotonically. This monotonic behavior of the $B_i(GT_+)$ values as a function of $B_1(E2)$ is also shown in fig. 1. The only slight deviation from a monotonic behavior occurs in ^{20}Ne for the value of $x = -1$ which corresponds to complete degeneracy in the single-particle spectrum. For comparison, in both tables and in fig. 1, the $B_1(E2)$ values for in the SU(3) model are also shown. As remarked earlier, in this limit, the total GT_+ strength is zero.

Note that the GT_+ strength from the ground state in ^{44}Ti to the lowest $J^\pi = 1^+$ state in ^{44}V , $B_1(GT_+)$, does not show the same monotonic behavior as the total strength does. We can see from table 2 that the change in the behavior of $B_1(GT_+)$ occurs around the point where the quadrupole moment Q changes sign and the nuclear shape changes from prolate to oblate.

Now we discuss the results for the ground state to ground state ($J^\pi = 0^+$, $T = 2 \rightarrow J^\pi = 0^+$, $T = 0$) double Gamow-Teller (DGT) transition amplitude, $A_1(\text{DGT})$. This is of interest to double-beta-decay calculations and possibly to double-charge-exchange

reactions with pions. The $A_1(\text{DGT})$ values for different choices of x are given in the rightmost column in tables 1 and 2. In fig. 2, we show the results for $A_1(\text{DGT})$ as a function of $B_1(E2)$. We see that when the Wildenthal [3] and the FPD6 [5] interactions are used for ^{20}Ne and ^{44}Ti , respectively, the DGT amplitude $A_1(\text{DGT})$ decreases monotonically with increasing $B_1(E2)$. This has been noted previously in ref. [7]. There, we also found that when the MKB interaction is used, $A_1(\text{DGT})$ as a function of the single particle splittings deviates slightly from the monotonic behavior for large values of x or small values of $B_1(E2)$. One can also see this non-monotonic behavior from table 2 and fig. 2. The complicated behavior of $A_1(\text{DGT})$ is not totally unexpected because it involves not only the lowest 1^+ state (in the intermediate nucleus) but all the 1^+ states.

Note that the DGT amplitude $A_1(\text{DGT})$ vanishes in both the SU(3) limit and the SU(4) limit, due to the vanishing of the total GT_+ and GT_- strengths from the final $N = Z$ nucleus.

Finally we discuss the results for the total M1

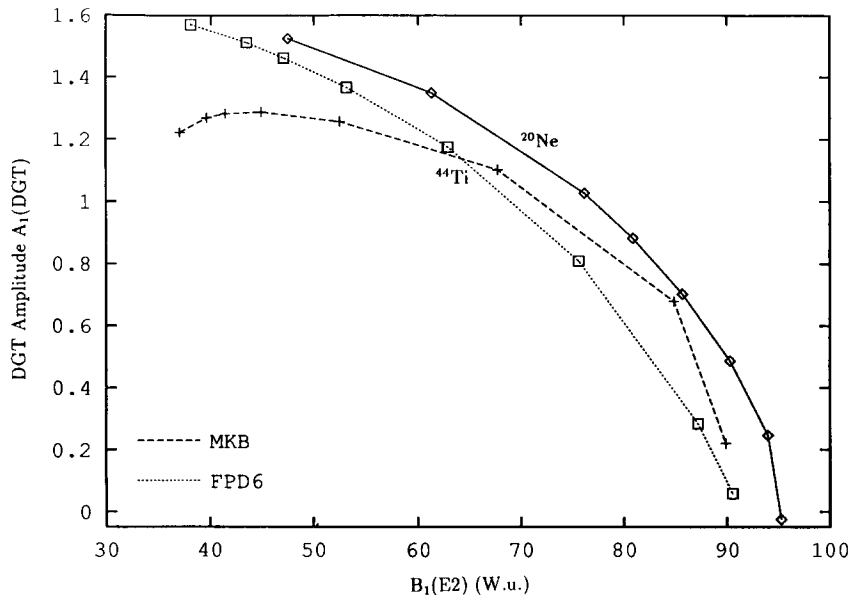


Fig. 2. The DGT transition amplitude from the $J^\pi = 0_1^+$, $T = 2$ state to the $J^\pi = 0_1^+$, $T = 0$ state as a function of the $B_1(E2)$ from the $J^\pi = 0_1^+$, $T = 0$ state to the $J^\pi = 2_1^+$, $T = 0$ state. The Wildenthal interaction was used for ^{20}Ne and the MKB and the FPD6 interactions were used for ^{44}Ti . The symbols “+”, “x”, “ Δ ”, etc. signify the points for which actual calculations were performed.

strength. In tables 1 and 2, we give the total spin, orbital and full M1 strengths [$B_s(M1)$, $B_o(M1)$ and $B_t(M1)$] for different values of x . The M1 strength to the lowest $J^\pi = 1^+$, $T = 1$ state, $B_1(M1)$, is also shown. From fig. 3, in which we plot the total spin and orbital M1 strengths as a function of $B_1(E2)$, it is evident that the total spin M1 strength decreases monotonically with increasing $B_1(E2)$, while the total orbital M1 strength increases monotonically with increasing $B_1(E2)$. The strong correlation between the total orbital M1 strength and the $B_1(E2)$ values has recently been well established experimentally [8,9]. There have been several theoretical works that associate orbital M1 strength with nuclear deformation [10–14]. That the total spin M1 strength decreases with increasing nuclear deformation has also been noted previously in refs. [14,15]. It was pointed out in ref. [15] that in the large deformation limit, the spin M1 strength vanishes. Note that the $B_1(M1)$ values in ^{44}Ti , which are for the transition to the lowest $J^\pi = 1^+$ state alone, are not monotonic with increasing $B_1(E2)$ (see table 2).

4. Further discussions

Let us return to the total GT_+ strength. The decrease of the total GT_+ strength $B_t(\text{GT}_+)$ as a function of the increasing $B_1(E2)$ values, is quite independent on the kind of interaction used as can be seen from table 2, where the results for ^{44}Ti are given for two effective interactions, the MKB [4] and the FPD6 [5]. We can also see this from fig. 1, in which the two curves for ^{44}Ti and the curve for ^{20}Ne have very similar shapes. These curves are also very similar to the curve obtained for the total GT_+ strength in ^{26}Mg , as described in ref. [1].

We should remark that the dependence of the total GT_+ strength on the $B_1(E2)$ values is not a single-valued function. This applies, in particular, to the small values of the GT_+ strength, i.e., when the quenching is very large. There are many models in which the $B_1(E2)$ values are different and which will give zero or nearly zero GT_+ values. For example, in the cartesian harmonic oscillator model for ^{20}Ne , the ground state wave function is given by the state in which the excess four nucleons occupy the orbit with

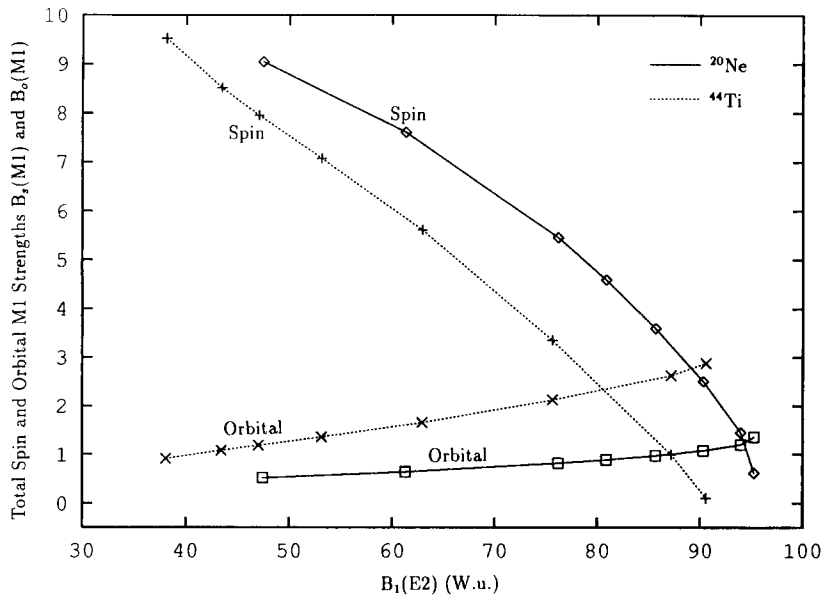


Fig. 3. The spin and orbital total M1 transition strengths from the ground states in ^{20}Ne and in ^{44}Ti as a function of the $B_1(E2)$ values from the ground state to the first excited $J^\pi = 2^+$ state. The Wildenthal interaction was used for ^{20}Ne and the FPD6 interaction was used for ^{44}Ti . The symbols “+”, “x”, “ \triangle ”, etc. signify the points for which actual calculations were performed.

($n_x = 0, n_y = 0, n_z = 2$). To form a final $J^\pi = 1^+$ state, one has to excite one of the nucleons in the intrinsic state to, say, ($n_x = 0, n_y = 1, n_z = 1$). The spin operator cannot change the spatial wave function. Thus the GT or spin M1 transition matrix elements are zero. However, the $B_1(E2)$ value obtained in this model is smaller than, for example, the $B_1(E2)$ value obtained from the SU(3) wave functions. Nevertheless, we believe that for larger values of the GT_+ strength, the correspondence between a given $B_1(E2)$ value and the total GT_+ strength is better defined and should provide us with a practical way to estimate the quenching of the GT_+ strength from the measured $B_1(E2)$ values. We base this conclusion on the fact that the curves shown in fig. 1 for ^{20}Ne and ^{44}Ti , as well as the results given in ref. [1], show a very similar, quite “universal” behavior.

We emphasize again that the quenching of the total GT_+ strength that we are addressing here applies also to the total GT_- strength in the same additive way. However, since most nuclei have a neutron excess and the total GT_- strength is usually much larger than the total GT_+ strength, our results are more useful in

estimating the quenching of the GT_+ strength in β_+ transitions.

Recently the total GT_+ strength was measured in the (n, p) reaction on ^{54}Fe and ^{56}Fe [16]. The total GT_+ strength found for ^{54}Fe is $B_1(GT_+) = 3.5$, while for ^{56}Fe , $B_1(GT_+) = 2.3$. The authors point out that these results are in agreement with the findings of ref. [1]. The $B_1(E2)$ value for ^{56}Fe is $620 e^2 \text{fm}^4$, larger than the $B_1(E2)$ value of $980 e^2 \text{fm}^4$ for ^{54}Fe [17] and, therefore, according to ref. [1] and the present work, the quenching of the total GT_+ strength should be larger in ^{56}Fe than in ^{54}Fe . This recent experimental work provides a nice example of the kind of use one can make of the relationship we have established in this work and in ref. [1].

Acknowledgement

We thank G.F. Bertsch for useful discussions and B.R. Barrett for a careful reading of the manuscript and discussions. One of us (D.C.Z.) thanks the Institute for Nuclear Theory at the University of Wash-

ington for its hospitality and support during his visit. This work was supported in part by the National Science Foundation under Grant No. PHY-90-17077 and Grant No. PHY-9103011 and by the Department of Energy under contract number DE-FG05-86ER-40299.

References

- [1] N. Auerbach, G.F. Bertsch, B.A. Brown and L. Zhao, β^+ Gamow-Teller strength in nuclei, to be published.
- [2] B.A. Brown and B.H. Wildenthal, *At. Data Nucl. Data Tables* 33 (1985) 347.
- [3] B.H. Wildenthal, *Prog. Part. Nucl. Phys.* 11 (1984) 5.
- [4] K. Muto and H. Horie, *Phys. Lett. B* 138 (1984) 9.
- [5] W.A. Richter, M.G. Van Der Merwe, R.E. Julies and B.A. Brown, *Nucl. Phys. A* 523 (1991) 325.
- [6] J.P. Elliott, *Proc. Roy. Soc. (London) A* 245 (1958) 128, 152.
- [7] D.C. Zheng, L. Zamick and N. Auerbach, *Ann. Phys. (NY)* 197 (1990) 343.
- [8] D. Bohle et al., *Phys. Lett. B* 137 (1987) 27.
- [9] W. Ziegler, C. Rangacharyulu, A. Richter and C. Spieler, *Phys. Rev. Lett.* 65 (1990) 2515; C. Rangacharyulu, A. Richter, H.J. Wörtche, W. Ziegler and R.F. Casten, *Phys. Rev. C* 43 (1991) R949.
- [10] N. LoIudice and F. Palumbo, *Phys. Rev. Lett.* 41 (1978) 1532; *Nucl. Phys. A* 236 (1978) 193.
- [11] F. Iachello, *Nucl. Phys. A* 358 (1981) 896.
- [12] A. Poves, J. Retamosa and E. Moya de Guerra, *Phys. Rev. C* 39 (1989) 1639; J. Retawosa, J.M. Udias, A. Poves and E. Moya de Guerra, *Nucl. Phys. A* 511 (1990) 221.
- [13] K. Heyde and C. De Coster, *Phys. Rev. C* 44 (1991) R2262.
- [14] L. Zamick and D.C. Zheng, *Phys. Rev. C* 44 (1991) 2522; *C* 46 (1992) 2106.
- [15] L. Zamick, D.C. Zheng and E. Moya de Guerra, *Phys. Rev. C* 39 (1989) 2370.
- [16] T. Ronnqvist et al., The $^{54,56}\text{Fe}(n, p)^{54,56}\text{Mn}$ reactions at $E_n = 97$ MeV, to be published.
- [17] S. Raman et al., *At. Data Nucl. Data Tables* 36 (1987) 1.